

Measurement of the absolute branching fraction of $D_{s0}^*(2317)^\pm \rightarrow \pi^0 D_s^\pm$

M. Ablikim¹, M. N. Achasov^{9,e}, S. Ahmed¹⁴, M. Albrecht⁴, A. Amoroso^{50A,50C}, F. F. An¹, Q. An^{47,a}, J. Z. Bai¹, O. Bakina²⁴, R. Baldini Ferroli^{20A}, Y. Ban³², D. W. Bennett¹⁹, J. V. Bennett⁵, N. Berger²³, M. Bertani^{20A}, D. Bettoni^{21A}, J. M. Bian⁴⁵, F. Bianchi^{50A,50C}, E. Boger^{24,c}, I. Boyko²⁴, R. A. Briere⁵, H. Cai⁵², X. Cai^{1,a}, O. Cakir^{42A}, A. Calcaterra^{20A}, G. F. Cao¹, S. A. Cetin^{42B}, J. Chai^{50C}, J. F. Chang^{1,a}, G. Chelkov^{24,c,d}, G. Chen¹, H. S. Chen¹, J. C. Chen¹, M. L. Chen^{1,a}, S. J. Chen³⁰, X. R. Chen²⁷, Y. B. Chen^{1,a}, X. K. Chu³², G. Cibinetto^{21A}, H. L. Dai^{1,a}, J. P. Dai^{35,j}, A. Dbeyssi¹⁴, D. Dedovich²⁴, Z. Y. Deng¹, A. Denig²³, I. Denysenko²⁴, M. Destefanis^{50A,50C}, F. De Mori^{50A,50C}, Y. Ding²⁸, C. Dong³¹, J. Dong^{1,a}, L. Y. Dong¹, M. Y. Dong^{1,a}, O. Dorjkhaidav²², Z. L. Dou³⁰, S. X. Du⁵⁴, P. F. Duan¹, J. Fang^{1,a}, S. S. Fang¹, X. Fang^{47,a}, Y. Fang¹, R. Farinelli^{21A,21B}, L. Fava^{50B,50C}, S. Fegan²³, F. Feldbauer²³, G. Felici^{20A}, C. Q. Feng^{47,a}, E. Fioravanti^{21A}, M. Fritsch^{14,23}, C. D. Fu¹, Q. Gao¹, X. L. Gao¹, Y. Gao⁴¹, Y. G. Gao⁶, Z. Gao^{47,a}, I. Garzia^{21A}, K. Goetzen¹⁰, L. Gong³¹, W. X. Gong^{1,a}, W. Gradl²³, M. Greco^{50A,50C}, M. H. Gu^{1,a}, S. Gu¹⁵, Y. T. Gu¹², A. Q. Guo¹, L. B. Guo²⁹, R. P. Guo¹, Y. P. Guo²³, Z. Haddadi²⁶, S. Han⁵², X. Q. Hao¹⁵, F. A. Harris⁴⁴, K. L. He¹, X. Q. He⁴⁶, F. H. Heinsius⁴, T. Held⁴, Y. K. Heng^{1,a}, T. Holtmann⁴, Z. L. Hou¹, C. Hu²⁹, H. M. Hu¹, T. Hu^{1,a}, Y. Hu¹, G. S. Huang^{47,a}, J. S. Huang¹⁵, X. T. Huang³⁴, X. Z. Huang³⁰, Z. L. Huang²⁸, T. Hussain⁴⁹, W. Ikegami Andersson⁵¹, Q. Ji¹, Q. P. Ji¹⁵, X. B. Ji¹, X. L. Ji^{1,a}, X. S. Jiang^{1,a}, X. Y. Jiang³¹, J. B. Jiao³⁴, Z. Jiao¹⁷, D. P. Jin^{1,a}, S. Jin¹, T. Johansson⁵¹, A. Julin⁴⁵, N. Kalantar-Nayestanaki²⁶, X. L. Kang¹, X. S. Kang³¹, M. Kavatsyuk²⁶, B. C. Ke⁵, T. Khan^{47,a}, P. Kiese²³, R. Kliemt¹⁰, L. Koch²⁵, O. B. Kolcu^{42B,h}, B. Kopf⁴, M. Kornicer⁴⁴, M. Kuemmel⁴, M. Kuhlmann⁴, A. Kupsc⁵¹, W. Kühn²⁵, J. S. Lange²⁵, M. Lara¹⁹, P. Larin¹⁴, L. Lavezzi^{50C,1}, H. Leithoff²⁴, C. Leng^{50C}, C. Li⁵¹, Cheng Li^{47,a}, D. M. Li⁵⁴, F. Li^{1,a}, F. Y. Li³², G. Li¹, H. B. Li¹, H. J. Li¹, J. C. Li¹, Jin Li³³, K. Li¹³, K. Li³⁴, Lei Li³, P. L. Li^{47,a}, P. R. Li^{7,43}, Q. Y. Li³⁴, T. Li³⁴, W. D. Li¹, W. G. Li¹, X. L. Li³⁴, X. N. Li^{1,a}, X. Q. Li³¹, Z. B. Li⁴⁰, H. Liang^{47,a}, Y. F. Liang³⁷, Y. T. Liang²⁵, G. R. Liao¹¹, D. X. Lin¹⁴, B. Liu^{35,j}, B. J. Liu¹, C. X. Liu¹, D. Liu^{47,a}, F. H. Liu³⁶, Fang Liu¹, Feng Liu⁶, H. B. Liu¹², H. H. Liu¹⁶, H. H. Liu¹, H. M. Liu¹, J. B. Liu^{47,a}, J. P. Liu⁵², J. Y. Liu¹, K. Liu⁴¹, K. Y. Liu²⁸, Ke Liu⁶, L. D. Liu³², P. L. Liu^{1,a}, Q. Liu⁴³, S. B. Liu^{47,a}, X. Liu²⁷, Y. B. Liu³¹, Y. Y. Liu³¹, Z. A. Liu^{1,a}, Zhiqing Liu²³, Y. F. Long³², X. C. Lou^{1,a,g}, H. J. Lu¹⁷, J. G. Lu^{1,a}, Y. Lu¹, Y. P. Lu^{1,a}, C. L. Luo²⁹, M. X. Luo⁵³, T. Luo⁴⁴, X. L. Luo^{1,a}, X. R. Lyu⁴³, F. C. Ma²⁸, H. L. Ma¹, L. L. Ma³⁴, M. M. Ma¹, Q. M. Ma¹, T. Ma¹, X. N. Ma³¹, X. Y. Ma^{1,a}, Y. M. Ma³⁴, F. E. Maas¹⁴, M. Maggiora^{50A,50C}, Q. A. Malik⁴⁹, Y. J. Mao³², Z. P. Mao¹, S. Marcello^{50A,50C}, J. G. Messchendorp²⁶, G. Mezzadri^{21B}, J. Min^{1,a}, T. J. Min¹, R. E. Mitchell¹⁹, X. H. Mo^{1,a}, Y. J. Mo⁶, C. Morales Morales¹⁴, G. Morello^{20A}, N. Yu. Muchnoi^{9,e}, H. Muramatsu⁴⁵, P. Musiol⁴, A. Mustafa⁴, Y. Nefedov²⁴, F. Nerling¹⁰, I. B. Nikolaev^{9,e}, Z. Ning^{1,a}, S. Nisar⁸, S. L. Niu^{1,a}, X. Y. Niu¹, S. L. Olsen³³, Q. Ouyang^{1,a}, S. Pacetti^{20B}, Y. Pan^{47,a}, P. Patteri^{20A}, M. Pelizaeus⁴, J. Pellegrino^{50A,50C}, H. P. Peng^{47,a}, K. Peters^{10,i}, J. Pettersson⁵¹, J. L. Ping²⁹, R. G. Ping¹, R. Poling⁴⁵, V. Prasad^{39,47}, H. R. Qi², M. Qi³⁰, S. Qian^{1,a}, C. F. Qiao⁴³, J. J. Qin⁴³, N. Qin⁵², X. S. Qin¹, Z. H. Qin^{1,a}, J. F. Qiu¹, K. H. Rashid⁴⁹, C. F. Redmer²³, M. Richter⁴, M. Ripka²³, G. Rong¹, Ch. Rosner¹⁴, X. D. Ruan¹², A. Sarantsev^{24,f}, M. Savrie^{21B}, C. Schmier⁴, K. Schoenning⁵¹, W. Shan³², M. Shao^{47,a}, C. P. Shen², P. X. Shen³¹, X. Y. Shen¹, H. Y. Sheng¹, J. J. Song³⁴, X. Y. Song¹, S. Sosio^{50A,50C}, C. Sowa⁴, S. Spataro^{50A,50C}, G. X. Sun¹, J. F. Sun¹⁵, S. S. Sun¹, X. H. Sun¹, Y. J. Sun^{47,a}, Y. K. Sun^{47,a}, Y. Z. Sun¹, Z. J. Sun^{1,a}, Z. T. Sun¹⁹, C. J. Tang³⁷, G. Y. Tang¹, X. Tang¹, I. Tapan^{42C}, M. Tiemens²⁶, B. T. Tsednee²², I. Uman^{42D}, G. S. Varner⁴⁴, B. Wang¹, B. L. Wang⁴³, D. Wang³², D. Y. Wang³², Dan Wang⁴³, K. Wang^{1,a}, L. L. Wang¹, L. S. Wang^{1,a}, M. Wang³⁴, P. Wang¹, P. L. Wang¹, W. P. Wang^{47,a}, X. F. Wang⁴¹, Y. D. Wang¹⁴, Y. F. Wang^{1,a}, Y. Q. Wang²³, Z. Wang^{1,a}, Z. G. Wang^{1,a}, Z. H. Wang^{47,a}, Z. Y. Wang¹, Z. Y. Wang¹, T. Weber²³, D. H. Wei¹¹, P. Weidenkaff²³, S. P. Wen¹, U. Wiedner⁴, M. Wolke⁵¹, L. H. Wu¹, L. J. Wu¹, Z. Wu^{1,a}, L. Xia^{47,a}, Y. Xia¹⁸, D. Xiao¹, H. Xiao⁴⁸, Y. J. Xiao¹, Z. J. Xiao²⁹, Y. G. Xie^{1,a}, Y. H. Xie⁶, X. A. Xiong¹, Q. L. Xiu^{1,a}, G. F. Xu¹, J. J. Xu¹, L. Xu¹, Q. J. Xu¹³, Q. N. Xu⁴³, X. P. Xu³⁸, L. Yan^{50A,50C}, W. B. Yan^{47,a}, W. C. Yan^{47,a}, Y. H. Yan¹⁸, H. J. Yang^{35,j}, H. X. Yang¹, L. Yang⁵², Y. H. Yang³⁰, Y. X. Yang¹¹, M. Ye^{1,a}, M. H. Ye⁷, J. H. Yin¹, Z. Y. You⁴⁰, B. X. Yu^{1,a}, C. X. Yu³¹, J. S. Yu²⁷, C. Z. Yuan¹, Y. Yuan¹, A. Yuncu^{42B,b}, A. A. Zafar⁴⁹, Y. Zeng¹⁸, Z. Zeng^{47,a}, B. X. Zhang¹, B. Y. Zhang^{1,a}, C. C. Zhang¹, D. H. Zhang¹, H. H. Zhang⁴⁰, H. Y. Zhang^{1,a}, J. Zhang¹, J. L. Zhang¹, J. Q. Zhang¹, J. W. Zhang^{1,a}, J. Y. Zhang¹, J. Z. Zhang¹, K. Zhang¹, L. Zhang⁴¹, S. Q. Zhang³¹, X. Y. Zhang³⁴, Y. Zhang¹, Y. Zhang¹, Y. H. Zhang^{1,a}, Y. T. Zhang^{47,a}, Yu Zhang⁴³, Z. H. Zhang⁶, Z. P. Zhang⁴⁷, Z. Y. Zhang⁵², G. Zhao¹, J. W. Zhao^{1,a}, J. Y. Zhao¹, J. Z. Zhao^{1,a}, Lei Zhao^{47,a}, Ling Zhao¹, M. G. Zhao³¹, Q. Zhao¹, S. J. Zhao⁵⁴, T. C. Zhao¹, Y. B. Zhao^{1,a}, Z. G. Zhao^{47,a}, A. Zhemchugov^{24,c}, B. Zheng^{14,48}, J. P. Zheng^{1,a}, W. J. Zheng³⁴, Y. H. Zheng⁴³, B. Zhong²⁹, L. Zhou^{1,a}, X. Zhou⁵², X. K. Zhou^{47,a}, X. R. Zhou^{47,a}, X. Y. Zhou¹, Y. X. Zhou^{12,a}, K. Zhu¹, K. J. Zhu^{1,a}, S. Zhu¹, S. H. Zhu⁴⁶, X. L. Zhu⁴¹, Y. C. Zhu^{47,a}, Y. S. Zhu¹, Z. A. Zhu¹, J. Zhuang^{1,a}, L. Zotti^{50A,50C}, B. S. Zou¹, J. H. Zou¹

(BESIII Collaboration)

¹ Institute of High Energy Physics, Beijing 100049, People's Republic of China² Beihang University, Beijing 100191, People's Republic of China³ Beijing Institute of Petrochemical Technology, Beijing 102617, People's Republic of China⁴ Bochum Ruhr-University, D-44780 Bochum, Germany⁵ Carnegie Mellon University, Pittsburgh, Pennsylvania 15213, USA⁶ Central China Normal University, Wuhan 430079, People's Republic of China⁷ China Center of Advanced Science and Technology, Beijing 100190, People's Republic of China⁸ COMSATS Institute of Information Technology, Lahore, Defence Road, Off Raiwind Road, 54000 Lahore, Pakistan⁹ G.I. Budker Institute of Nuclear Physics SB RAS (BINP), Novosibirsk 630090, Russia¹⁰ GSI Helmholtzcentre for Heavy Ion Research GmbH, D-64291 Darmstadt, Germany¹¹ Guangxi Normal University, Guilin 541004, People's Republic of China¹² Guangxi University, Nanning 530004, People's Republic of China¹³ Hangzhou Normal University, Hangzhou 310036, People's Republic of China¹⁴ Helmholtz Institute Mainz, Johann-Joachim-Becher-Weg 45, D-55099 Mainz, Germany¹⁵ Henan Normal University, Xinxiang 453007, People's Republic of China¹⁶ Henan University of Science and Technology, Luoyang 471003, People's Republic of China

- ¹⁷ Huangshan College, Huangshan 245000, People's Republic of China
¹⁸ Hunan University, Changsha 410082, People's Republic of China
¹⁹ Indiana University, Bloomington, Indiana 47405, USA
²⁰ (A)INFN Laboratori Nazionali di Frascati, I-00044, Frascati, Italy; (B)INFN and University of Perugia, I-06100, Perugia, Italy
²¹ (A)INFN Sezione di Ferrara, I-44122, Ferrara, Italy; (B)University of Ferrara, I-44122, Ferrara, Italy
²² Institute of Physics and Technology, Peace Ave. 54B, Ulaanbaatar 13330, Mongolia
²³ Johannes Gutenberg University of Mainz, Johann-Joachim-Becher-Weg 45, D-55099 Mainz, Germany
²⁴ Joint Institute for Nuclear Research, 141980 Dubna, Moscow region, Russia
²⁵ Justus-Liebig-Universität Giessen, II. Physikalisches Institut, Heinrich-Buff-Ring 16, D-35392 Giessen, Germany
²⁶ KVI-CART, University of Groningen, NL-9747 AA Groningen, The Netherlands
²⁷ Lanzhou University, Lanzhou 730000, People's Republic of China
²⁸ Liaoning University, Shenyang 110036, People's Republic of China
²⁹ Nanjing Normal University, Nanjing 210023, People's Republic of China
³⁰ Nanjing University, Nanjing 210093, People's Republic of China
³¹ Nankai University, Tianjin 300071, People's Republic of China
³² Peking University, Beijing 100871, People's Republic of China
³³ Seoul National University, Seoul, 151-747 Korea
³⁴ Shandong University, Jinan 250100, People's Republic of China
³⁵ Shanghai Jiao Tong University, Shanghai 200240, People's Republic of China
³⁶ Shanxi University, Taiyuan 030006, People's Republic of China
³⁷ Sichuan University, Chengdu 610064, People's Republic of China
³⁸ Soochow University, Suzhou 215006, People's Republic of China
³⁹ State Key Laboratory of Particle Detection and Electronics, Beijing 100049, Hefei 230026, People's Republic of China
⁴⁰ Sun Yat-Sen University, Guangzhou 510275, People's Republic of China
⁴¹ Tsinghua University, Beijing 100084, People's Republic of China
⁴² (A)Ankara University, 06100 Tandogan, Ankara, Turkey; (B)Istanbul Bilgi University, 34060 Eyup, Istanbul, Turkey;
(C)Uludag University, 16059 Bursa, Turkey; (D)Near East University, Nicosia, North Cyprus, Mersin 10, Turkey
⁴³ University of Chinese Academy of Sciences, Beijing 100049, People's Republic of China
⁴⁴ University of Hawaii, Honolulu, Hawaii 96822, USA
⁴⁵ University of Minnesota, Minneapolis, Minnesota 55455, USA
⁴⁶ University of Science and Technology Liaoning, Anshan 114051, People's Republic of China
⁴⁷ University of Science and Technology of China, Hefei 230026, People's Republic of China
⁴⁸ University of South China, Hengyang 421001, People's Republic of China
⁴⁹ University of the Punjab, Lahore-54590, Pakistan
⁵⁰ (A)University of Turin, I-10125, Turin, Italy; (B)University of Eastern Piedmont, I-15121, Alessandria, Italy; (C)INFN, I-10125, Turin, Italy
⁵¹ Uppsala University, Box 516, SE-75120 Uppsala, Sweden
⁵² Wuhan University, Wuhan 430072, People's Republic of China
⁵³ Zhejiang University, Hangzhou 310027, People's Republic of China
⁵⁴ Zhengzhou University, Zhengzhou 450001, People's Republic of China
^a Also at State Key Laboratory of Particle Detection and Electronics, Beijing 100049, Hefei 230026, People's Republic of China
^b Also at Bogazici University, 34342 Istanbul, Turkey
^c Also at the Moscow Institute of Physics and Technology, Moscow 141700, Russia
^d Also at the Functional Electronics Laboratory, Tomsk State University, Tomsk, 634050, Russia
^e Also at the Novosibirsk State University, Novosibirsk, 630090, Russia
^f Also at the NRC Kurchatov Institute, PNPI, 188300, Gatchina, Russia
^g Also at University of Texas at Dallas, Richardson, Texas 75083, USA
^h Also at Istanbul Arel University, 34295 Istanbul, Turkey
ⁱ Also at Goethe University Frankfurt, 60323 Frankfurt am Main, Germany
^j Also at Key Laboratory for Particle Physics, Astrophysics and Cosmology, Ministry of Education; Shanghai Key Laboratory for Particle Physics and Cosmology; Institute of Nuclear and Particle Physics, Shanghai 200240, People's Republic of China

(Dated: March 25, 2022)

The process $e^+e^- \rightarrow D_s^{*+}D_{s0}^*(2317)^- + c.c.$ is observed for the first time with the data sample of 567 pb^{-1} collected with the BESIII detector operating at the BEPCII collider at a center-of-mass energy $\sqrt{s} = 4.6 \text{ GeV}$. The statistical significance of the $D_{s0}^*(2317)^\pm$ signal is 5.8σ and the mass is measured to be $(2318.3 \pm 1.2 \pm 1.2) \text{ MeV}/c^2$. The absolute branching fraction $\mathcal{B}(D_{s0}^*(2317)^\pm \rightarrow \pi^0 D_s^\pm)$ is measured as $1.00_{-0.14}^{+0.00} \pm 0.14$ for the first time. The uncertainties are statistical and systematic, respectively.

PACS numbers: 13.25.Ft, 13.66.Bc, 14.40.Lb, 14.40.Rt.

The $D_{s0}^*(2317)^-$ meson was first observed at the BABAR experiment via its decay to $\pi^0 D_s^-$ [1, 2]; it was subsequently

confirmed at the CLEO [3] and Belle [4] experiments. The $D_{s0}^*(2317)^-$ meson is suggested to be the P -wave $\bar{c}s$ state

with spin-parity $J^P = 0^+$. However, the measured mass (2317.7 ± 0.6) MeV/ c^2 [5] is at least 150 MeV/ c^2 lower than the calculations of a potential model [6] and lattice QCD [7] for such a state. As the $D_{s_0}^*(2317)^-$ is 45 MeV/ c^2 below the DK threshold, it has been proposed as a good candidate for a DK molecule [8], a $\bar{c}s q \bar{q}$ tetraquark state [9], or a mixture of a $\bar{c}s$ meson and a $\bar{c}s q \bar{q}$ tetraquark [10].

The $D_{s_0}^*(2317)^-$ is extremely narrow, and the upper limit on its width is 3.8 MeV at the 95% confidence level (C.L.) [11]. The only known decay is the isospin-violating mode $\pi^0 D_s^-$, and no branching fraction or partial width of this mode has been measured. Theoretical calculations give different values for the partial decay width $\Gamma(D_{s_0}^*(2317)^- \rightarrow \pi^0 D_s^-)$ based on different assumptions [12–15]. The partial width $\Gamma(D_{s_0}^*(2317)^- \rightarrow \pi^0 D_s^-)$ is around 30 keV or even as low as a few keV if the $D_{s_0}^*(2317)^-$ is a pure $\bar{c}s$ state, while it can be enhanced by a hundred keV or even larger in the molecule picture due to the contribution of meson loops. Therefore, the partial decay width or the branching fraction is a key quantity to identify the nature of the $D_{s_0}^*(2317)^-$.

In this Letter, we present first observation of $e^+e^- \rightarrow D_s^{*+} D_{s_0}^*(2317)^- + c.c.$ and the first measurement of the absolute branching fraction of $D_{s_0}^*(2317)^- \rightarrow \pi^0 D_s^-$. Throughout the text, the inclusion of the charge conjugate mode is implied unless otherwise stated. The data sample, which corresponds to an integrated luminosity of 567 pb $^{-1}$ [16], is collected at a center-of-mass (c.m.) energy of 4.6 GeV [17] with the BESIII detector [18] operating at the BEPCII collider [19]. In this analysis, a D_s^{*+} is reconstructed via its γD_s^+ decay with D_s^+ decaying to $K^+ K^- \pi^+$, and its recoil mass spectrum is examined to search for a $D_{s_0}^*(2317)^-$ signal. The D_s^{*+} tagged sample is further divided into two subcategories, one with a tagged π^0 and the other with no tagged π^0 . By using the numbers of signal events in these two categories, the absolute branching fraction of $D_{s_0}^*(2317)^- \rightarrow \pi^0 D_s^-$ is determined.

In order to determine the detection efficiency and to optimize the selection criteria, the GEANT4-based [20] Monte Carlo (MC) simulation software BOOST [21], which includes the geometric description of the detector and detector responses, is used to simulate $e^+e^- \rightarrow D_s^{*+} D_{s_0}^*(2317)^-$ at $\sqrt{s} = 4.6$ GeV with $D_s^{*+} \rightarrow \gamma D_s^+$ and $D_s^+ \rightarrow K^+ K^- \pi^+$, and $D_{s_0}^*(2317)^- \rightarrow \pi^0 D_s^-$ or γD_s^{*-} . The D_s^- and D_s^{*-} are set to decay inclusively. The J^P of $D_{s_0}^*(2317)^-$ is 0^+ , so it is in relative S -wave to the D_s^{*+} , and they are generated uniformly in phase space. The initial state radiation (ISR) is simulated with KKMC [22] using a calculation with a precision better than 0.2%. The final state radiation (FSR) effects associated with charged particles is handled with PHOTOS [23]. To study the possible backgrounds, an inclusive MC sample with an integrated luminosity equivalent to data is generated. All the known charmonium transitions, hadronic decays and open charm channels are modeled with EVTGEN [24, 25] incorporating the branching fractions taken from the Particle Data Group [5], while the QED processes and the unknown

charmonium decays are generated with BABAYAGA [26] and LUNDCHARM [27], respectively.

To reconstruct D_s^{*+} , the γD_s^+ channel is used with D_s^+ decaying to $K^+ K^- \pi^+$. Events with at least three charged track candidates and at least one photon candidate are selected. For each charged track candidate, the polar angle θ in the multi-layer drift chamber (MDC) must satisfy $|\cos\theta| < 0.93$, and the distance of the closest approach to the e^+e^- interaction point is required to be less than 10 cm along the beam direction and less than 1 cm in the plane perpendicular to the beam. Particle identification (PID), which uses both the information from time of flight (TOF) and the specific energy loss (dE/dx), is performed to separate kaons and pions. The photon candidates are selected from showers in the electromagnetic calorimeter (EMC) with deposited energy greater than 25 MeV in the barrel ($|\cos(\theta)| < 0.8$), or greater than 50 MeV in the end-cap regions ($0.86 < |\cos(\theta)| < 0.92$). To eliminate showers produced by charged tracks, the photon candidate must be separated by at least 20 degrees from any charged track. The time for the shower measured by the EMC from the start of this event is restricted to be less than 700 ns to suppress electronic noise and energy depositions unrelated to the event.

All combinations are required to have the invariant masses of $K^+ K^- \pi^+$ and $\gamma K^+ K^- \pi^+$ within $\Delta M_{K^+ K^- \pi^+} \equiv |M(K^+ K^- \pi^+) - m_{D_s^+}| < 16$ MeV/ c^2 and $\Delta M_{\gamma K^+ K^- \pi^+} \equiv |M(\gamma K^+ K^- \pi^+) - m_{D_s^{*+}}| < 11$ MeV/ c^2 , where $M((\gamma)K^+ K^- \pi^+)$ is the invariant mass of the $(\gamma)K^+ K^- \pi^+$ system and $m_{D_s^+}/m_{D_s^{*+}}$ is the nominal mass of D_s^+/D_s^{*+} [5]. A two-constraint (2C) kinematic fit is performed on the surviving events with the mass constraints of D_s and D_s^* to obtain a better recoil mass resolution and to suppress backgrounds. The χ_{2C}^2 from the kinematic fit is required to be less than 14. All successful combinations in each event are kept for further study.

After the previously described selection criteria, the recoil mass distribution of D_s^{*+} is shown in Fig. 1, where a $D_{s_0}^*(2317)^-$ signal can be observed. The events in the sidebands of D_s^+ and D_s^{*+} in the sample before the kinematic fit are checked and no signal of $D_{s_0}^*(2317)^-$ is observed. The inclusive MC sample, which does not include production of the $D_{s_0}^*(2317)^-$, matches well with the background from data. In the inclusive MC sample, the remaining events are non- D_s^{*+} events around the $D_{s_0}^*(2317)^-$ peak, including non- D_s^+ events and mis-combined γD_s^+ events, where the γ or D_s^+ could come from other decay modes of D_s^{*+} . For the event with a real D_s^{*+} , such as $e^+e^- \rightarrow D_s^{*+} D_s^{*-}$ or $D_s^{*+} D_s^-$, the recoil mass of D_s^{*+} is far away from the $D_{s_0}^*(2317)^-$ peak and has no influence in this analysis. In general, none of the known backgrounds can form a peak in the signal region. On the other hand, the technique to measure the absolute branching fraction $\mathcal{B}(D_{s_0}^*(2317)^- \rightarrow \pi^0 D_s^-)$ avoids the influence of the unknown three-body processes $\gamma D_s^+ D_{s_0}^*(2317)^-$ and $\pi^0 D_s^+ D_{s_0}^*(2317)^-$ even if they exist

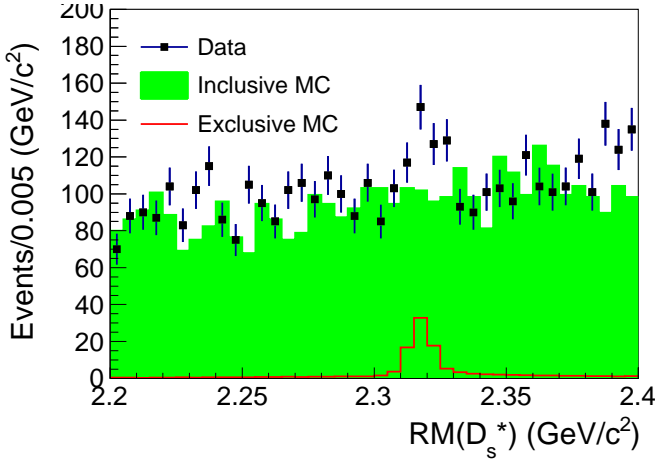


FIG. 1: (Color online) Distribution of the D_s^{*+} recoil mass of the events from data (black dots) and inclusive MC sample (green histogram), which is normalized according to the integrated luminosity. The red curve shows the same distribution for $D_s^{*+}D_{s_0}^*(2317)^-$ events from MC simulation.

since they have an identical $D_{s_0}^*(2317)^-$ compared to the signal process $D_s^{*+}D_{s_0}^*(2317)^-$.

The process $e^+e^- \rightarrow D_s^{*+}D_{s_0}^*(2317)^- \rightarrow D_s^{*+}\pi^0 D_s^-$ is studied via a further π^0 reconstruction with two photons from the remaining showers in the EMC and D_s^- as missing particle. If there are more than two photons, all combinations of $\gamma\gamma D_s^{*+}$ are subjected to a 4C kinematic fit with mass constraints on the D_s^+ , D_s^{*+} , π^0 candidates and a missing D_s^- , requiring the χ_{4C}^2 to be less than 36.

The requirements on $\Delta M_{K^+K^-\pi^+}$, $\Delta M_{\gamma K^+K^-\pi^+}$, χ_{2C}^2 and χ_{4C}^2 are optimized with MC samples to obtain the best statistical precision of $\mathcal{B}(D_{s_0}^*(2317)^- \rightarrow \pi^0 D_s^-)$. The $D_s^{*+}D_{s_0}^*(2317)^-$ signal is generated by assuming $\mathcal{B}(D_{s_0}^*(2317)^- \rightarrow \pi^0 D_s^-) = 0.9$ and $\mathcal{B}(D_{s_0}^*(2317)^- \rightarrow \gamma D_s^{*-}) = 0.1$ and normalized according to the number of signal events from data. The background is taken from a toy MC sample generated by fitting the recoil mass distribution of D_s^{*+} from data. The MC samples are analyzed with the same procedure as for data to obtain the branching fraction $\mathcal{B}(D_{s_0}^*(2317)^- \rightarrow \pi^0 D_s^-)$. The requirements yielding the smallest relative statistical uncertainty are used in this analysis.

The $e^+e^- \rightarrow D_s^{*+}D_{s_0}^*(2317)^-$ events are divided in two subcategories: “ π^0 -tag succeeded” if at least one π^0 is tagged and the event passed the 4C kinematic fit, and “ π^0 -tag failed” for the other events. The recoil mass distributions of the D_s^{*+} from the 2C kinematic fit of these two subcategories are shown in Fig. 2. These distributions are fitted simultaneously to measure the branching fraction of $D_{s_0}^*(2317)^- \rightarrow \pi^0 D_s^-$.

The real $D_{s_0}^*(2317)^- \rightarrow \pi^0 D_s^-$ signal events could be categorized into both subsamples since the detection efficiency for π^0 is 43.4%. On the other hand, potential background events, such as $D_{s_0}^*(2317)^- \rightarrow \gamma D_s^{*-}$ or other decay chan-

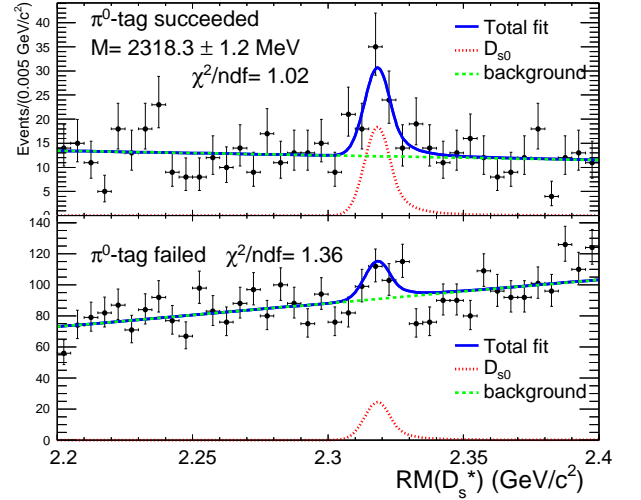


FIG. 2: (Color online) Fit result for data at 4.6 GeV for the two subsamples, “ π^0 -tag succeeded” (top) and “ π^0 -tag failed” (bottom). The red dotted and green dashed curves show the fit results for signal and background, respectively, while the blue curve shows their sum.

nels, could be reconstructed in the “ π^0 -tag succeeded” sample too. Therefore, the number of $D_{s_0}^*(2317)^-$ signal events in the “ π^0 -tag succeeded” subsample, N_0 , is expressed as

$$N_0 = N_{\text{tot}}/\epsilon_{\text{tot}} \cdot \mathcal{B} \cdot \epsilon_{\text{sig}} + N_{\text{tot}}/\epsilon_{\text{tot}} \cdot (1 - \mathcal{B}) \cdot \epsilon_{\text{bkg}}, \quad (1)$$

where the first and the second terms represent the contributions from $D_{s_0}^*(2317)^- \rightarrow \pi^0 D_s^-$ (with a branching fraction of \mathcal{B}) and from the other $D_{s_0}^*(2317)^-$ decay mode (with a branching fraction of $1 - \mathcal{B}$), respectively. Here the other decay mode means the potential peaking background mode $D_{s_0}^*(2317)^- \rightarrow \gamma D_s^{*-}$, which is expected to be the dominant mode besides $\pi^0 D_s^-$, and any other decay modes are considered in the systematic uncertainty. The N_{tot} is the number of $D_{s_0}^*(2317)^-$ signal events in the full sample (the sum of “ π^0 -tag succeeded” and “ π^0 -tag failed” events), ϵ_{tot} is the corresponding detection efficiency for the reconstructed D_s^{*+} , $N_{\text{tot}}/\epsilon_{\text{tot}}$ is the number of produced $D_s^{*+}D_{s_0}^*(2317)^-$ events, ϵ_{sig} is the detection efficiency for $D_{s_0}^*(2317)^- \rightarrow \pi^0 D_s^-$ events being reconstructed in the “ π^0 -tag succeeded” sample including the branching fraction of $\pi^0 \rightarrow \gamma\gamma$ [5], and ϵ_{bkg} is the efficiency for non- $(D_{s_0}^*(2317)^- \rightarrow \pi^0 D_s^-)$ events to be reconstructed in the “ π^0 -tag succeeded” sample. The efficiencies ϵ_{tot} , ϵ_{sig} and ϵ_{bkg} are obtained from MC simulations, and are 40.0%, 17.2%, and 5.8%, respectively.

From Eq. (1), we derive the absolute branching fraction $\mathcal{B}(D_{s_0}^*(2317)^- \rightarrow \pi^0 D_s^-)$ as

$$\mathcal{B} = \frac{N_0 - N_{\text{tot}}/\epsilon_{\text{tot}} \cdot \epsilon_{\text{bkg}}}{N_{\text{tot}}/\epsilon_{\text{tot}} \cdot (\epsilon_{\text{sig}} - \epsilon_{\text{bkg}})}, \quad (2)$$

where the branching fraction \mathcal{B} and N_{tot} are the free parameters in a simultaneous fit to the recoil mass distributions of the D_s^{*+} in Fig. 2, and N_0 is calculated using Eq. (1).

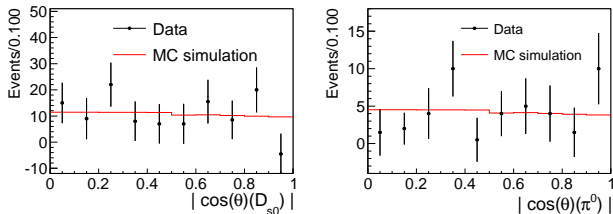


FIG. 3: (Color online) Angular distributions of $D_{s_0}^*(2317)^-$ in the e^+e^- c.m. system (left) and of π^0 in the $D_{s_0}^*(2317)^-$ c.m. system (right). Black dots and red lines represent the data after background subtraction and MC simulation, respectively.

The shape for the $D_{s_0}^*(2317)^-$ signal is described with a Crystal Ball function [28] convolved with a Gaussian function, while the background is parameterized with a linear function. The parameters of the Crystal Ball function except for the mass are fixed to the values from a fit to the MC simulated $D_s^{*+}D_{s_0}^*(2317)^-$ sample, in which the $D_{s_0}^*(2317)^-$ is simulated with zero width. The Gaussian function is used to describe the data-MC difference in mass resolution, and the standard deviation is taken from a control sample of $e^+e^- \rightarrow D_s^{*+}D_s^{*-}$ at 4.6 GeV. By reconstructing the D_s^{*+} from the process $e^+e^- \rightarrow D_s^{*+}D_s^{*-}$, it is found that the recoiling D_s^{*+} signal shape in MC simulation needs to be smeared by a Gaussian with the standard deviation of 0.9 MeV/ c^2 in order to match the data. The standard deviation of the Gaussian function in the fit to the $D_{s_0}^*(2317)^-$ signal is fixed to this value.

From the simultaneous fit, the total number of $D_{s_0}^*(2317)^-$ signal events is 115 ± 21 , and the number of $D_{s_0}^*(2317)^-$ events in the “ π^0 tag-succeed” subsample is 46.8 ± 9.4 . The latter event yield is found to be 49.3 with a constraint that the branching fraction is no larger than one. Using Eq. (2), the absolute branching fraction of $D_{s_0}^*(2317)^- \rightarrow \pi^0 D_s^-$ is measured to be $1.00_{-0.14}^{+0.00}$, with a constraint that the branching fraction cannot be larger than one. The statistical uncertainty, 0.14, is estimated by covering 68.3% confidence level from the likelihood distribution of the branching fraction. By comparing the difference of the log-likelihood with and without the $D_{s_0}^*(2317)^-$ signal in the fit and considering the change of the number of degrees of freedom, the statistical significance of the $D_{s_0}^*(2317)^-$ signal is estimated as 5.8σ . The mass of $D_{s_0}^*(2317)^-$ is measured to be (2318.3 ± 1.2) MeV/ c^2 .

The J^P of $D_{s_0}^*(2317)$ is 0^+ , so both the $D_s^{*+}D_{s_0}^*(2317)^-$ and the $\pi^0 D_s^-$ systems are expected to be in a relative S -wave, and the angular distributions are expected to be flat. We define the signal region of $D_{s_0}^*(2317)^-$ as $[2.31, 2.33]$ GeV/ c^2 , and the sideband regions as $[2.28, 2.30]$ and $[2.34, 2.36]$ GeV/ c^2 to estimate the contribution of background. Figure 3 shows the angular distributions of $D_{s_0}^*(2317)^-$ in the e^+e^- c.m. system and of π^0 in the $D_{s_0}^*(2317)^-$ c.m. system. Both distributions are flat as expected, and can be modeled by the MC simulations.

For the branching fraction measurement, many sources of

systematic uncertainties cancel since the branching fraction is determined by the relative signal yields in the two subsamples. The main systematic uncertainties come from π^0 reconstruction, the used signal and background shapes, $\pi^0 D_s^-$ selections, the possible width of $D_{s_0}^*(2317)^-$, and potential peaking backgrounds.

The uncertainty on π^0 reconstruction is taken as 0.7% from a study of $\psi(3686) \rightarrow J/\psi\pi^0\pi^0$ and $e^+e^- \rightarrow \omega\pi^0$ by considering the momentum dependency of π^0 . In the nominal fit, the signal shape is parameterized by a Crystal Ball function with a tail due to the ISR effect. Given that the energy dependent cross sections of $e^+e^- \rightarrow D_s^{*+}D_{s_0}^*(2317)^-$ are not measured with high precision, the systematic uncertainty should be studied conservatively. We vary the signal shape to a Gaussian with all parameters free, and the relative difference in the branching fractions, 5.0%, is taken as systematic uncertainty. The background in the nominal fit is parameterized as a linear function. We change this shape to a second order polynomial function and take the relative difference in branching fractions, 7.4%, as systematic uncertainty due to background shape.

For $\pi^0 D_s^-$ selection, we perform a kinematic fit, which could cause a systematic bias in the efficiency between data and MC simulation. To study this difference, we correct the helix parameters of the charged tracks in MC simulation [29], the difference in χ^2 distribution between data and MC simulation becomes negligibly small according to other studies [30]. We take half of the difference in the ratio of detection efficiencies ϵ_{sig} and ϵ_{tot} between MC simulations with and without this correction as systematic uncertainty (3.1%). The nominal result is based on the corrected MC simulation.

The width of $D_{s_0}^*(2317)$ is unknown and cannot be measured in this analysis due to limited statistics. In the nominal fit, we use the shape from MC simulation of $D_{s_0}^*(2317)^-$ with a zero width to describe the signal. The upper limit on the width of $D_{s_0}^*(2317)^-$ is estimated as 3.8 MeV at 95% C.L. from previous experiments [5]. In an alternative fit, we change the width of $D_{s_0}^*(2317)^-$ to 3.8 MeV and use the same Gaussian function to convolve the shape from MC simulation, and take the difference in the branching fraction, 5.3%, as systematic uncertainty.

In Eq. (2), the peaking background is considered, and the result of the fit shows that its contribution is negligible. For the signal mode, $D_{s_0}^*(2317)^- \rightarrow \pi^0 D_s^-$, the tagged π^0 could also come from D_s^- . This kind of events is regarded as signal, and its contribution is included in the definition of the efficiency, which is estimated from the MC simulation of $e^+e^- \rightarrow D_s^{*+}D_{s_0}^*(2317)^- \rightarrow D_s^{*+}\pi^0 D_s^-$ with D_s^- decaying to all possible modes. All peaking backgrounds come from other decay modes of $D_{s_0}^*(2317)^-$. To study the possible contribution conservatively, we simulate the potential peaking backgrounds, $D_{s_0}^*(2317)^- \rightarrow \gamma D_s^{*-}$, $\gamma\gamma D_s^-$ and $\pi^+\pi^- D_s^-$ exclusively. The upper limits on the ratio $\Gamma(\gamma D_s^{*-})/\Gamma(\pi^0 D_s^-)$, $\Gamma(\gamma\gamma D_s^-)/\Gamma(\pi^0 D_s^-)$, and $\Gamma(\pi^+\pi^- D_s^-)/\Gamma(\pi^0 D_s^-)$, are esti-

mated as 0.059, 0.18, and 0.006 [5]. The total systematic uncertainty in $\mathcal{B}(D_{s0}^*(2317)^- \rightarrow \pi^0 D_s^-)$ is conservatively estimated to be 8.5%.

All the above systematic uncertainties are listed in Table I. Assuming all of them are independent and adding them in quadrature, we estimate a total systematic uncertainty of 13.8% in the branching fraction.

TABLE I: Summary of relative systematic uncertainties in $\mathcal{B}(D_{s0}^*(2317)^- \rightarrow \pi^0 D_s^-)$.

Source	Uncertainty (%)
π^0 reconstruction	0.7
Signal shape	5.0
Background shape	7.4
$\pi^0 D_s^-$ selections	3.1
Width of $D_{s0}^*(2317)^-$	5.3
Peaking backgrounds	8.5
Total	13.8

The systematic uncertainties in the mass measurement of $D_{s0}^*(2317)^-$ come from mass calibration, signal shape, background shape, and c.m. energy determination. For the mass calibration, we use the control sample $e^+e^- \rightarrow D_s^{*+}D_s^{*-}$ at 4.6 GeV and compare the mass of the recoiling D_s^{*-} with the world average value [5]. The same event selections and fit procedure as for $D_s^{*+}D_{s0}^*(2317)^-$ are used for $D_s^{*+}D_s^{*-}$, and the shape of the missing D_s^{*-} is parameterized as a Crystal Ball function convolved with a Gaussian function. The difference in the mass of D_s^{*-} between data and the world average value [5], which includes the contribution of the uncertainty on c.m. energy, 1.2 MeV/c², is taken as systematic uncertainty. The uncertainties in signal and background shapes are studied with the same method as for the systematic uncertainty study in branching fraction measurement. The results show that these systematic uncertainties are negligible.

In summary, we observe the $D_{s0}^*(2317)^-$ signal in the process $e^+e^- \rightarrow D_s^{*+}D_{s0}^*(2317)^-$ from a data sample at c.m. energy of 4.6 GeV. The statistical significance of $D_{s0}^*(2317)^-$ signal is 5.8σ , and the mass is determined to be $(2318.3 \pm 1.2 \pm 1.2)$ MeV/c². The absolute branching fraction of $D_{s0}^*(2317)^- \rightarrow \pi^0 D_s^-$ is measured for the first time to be $1.00_{-0.14}^{+0.00} \pm 0.14$, where the uncertainties are statistical and systematic, respectively. The result shows that the $D_{s0}^*(2317)^-$ tends to have a significantly smaller branching fraction to γD_s^{*-} than to $\pi^0 D_s^-$, and this differs from the expectation of the conventional $\bar{c}s$ hypothesis of the $D_{s0}^*(2317)^-$ [12] but agrees well with the calculation in the molecule picture [13]. In the future, with more data accumulated at BESIII or a fine scan from PANDA [31], the width of $D_{s0}^*(2317)^-$ could be measured. Combined with the absolute branching fractions of $D_{s0}^*(2317)^- \rightarrow \pi^0 D_s^-$ and γD_s^{*-} , we may shed light on the nature of the $D_{s0}^*(2317)^-$.

The BESIII collaboration thanks the staff of BEPCII and

the IHEP computing center for their strong support. This work is supported in part by National Key Basic Research Program of China under Contract No. 2015CB856700; National Natural Science Foundation of China (NSFC) under Contracts Nos. 11235011, 11322544, 11335008, 11425524, 11635010; the Chinese Academy of Sciences (CAS) Large-Scale Scientific Facility Program; the CAS Center for Excellence in Particle Physics (CCEPP); the Collaborative Innovation Center for Particles and Interactions (CICPI); Joint Large-Scale Scientific Facility Funds of the NSFC and CAS under Contracts Nos. U1632106, U1232201, U1332201, U1532257, U1532258; CAS under Contracts Nos. KJCX2-YW-N29, KJCX2-YW-N45; 100 Talents Program of CAS; National 1000 Talents Program of China; INPAC and Shanghai Key Laboratory for Particle Physics and Cosmology; German Research Foundation DFG under Contracts Nos. Collaborative Research Center CRC 1044, FOR 2359; Istituto Nazionale di Fisica Nucleare, Italy; Koninklijke Nederlandse Akademie van Wetenschappen (KNAW) under Contract No. 530-4CDP03; Ministry of Development of Turkey under Contract No. DPT2006K-120470; National Natural Science Foundation of China (NSFC) under Contract No. 11575133; National Science and Technology fund; NSFC under Contract No. 11275266; The Swedish Resarch Council; U. S. Department of Energy under Contracts Nos. DE-FG02-05ER41374, DE-SC-0010504, DE-SC0012069; University of Groningen (RuG) and the Helmholtzzentrum fuer Schwerionenforschung GmbH (GSI), Darmstadt; WCU Program of National Research Foundation of Korea under Contract No. R32-2008-000-10155-0; New Century Excellent Talents in University (NCET) under Contract No. NCET-13-0342; Shandong Natural Science Funds for Distinguished Young Scholar under Contract No. JQ201402.

-
- [1] B. Aubert *et al.* (BABAR Collaboration), Phys. Rev. Lett. **90**, 242001 (2003).
 - [2] B. Aubert *et al.* (BABAR Collaboration), Phys. Rev. Lett. **93**, 181801 (2004).
 - [3] D. Besson *et al.* (CLEO Collaboration), Phys. Rev. D **68**, 032002 (2003).
 - [4] P. Krokovny *et al.* (Belle Collaboration), Phys. Rev. Lett. **91**, 262002 (2003).
 - [5] C. Patrignani *et al.* (Particle Data Group), Chin. Phys. C **40**, 100001 (2016).
 - [6] S. Godfrey and N. Isgur, Phys. Rev. D **32**, 189 (1985); S. Godfrey and R. Kokoski, Phys. Rev. D **43**, 1679 (1991); J. Zeng, J. W. Van Orden and W. Roberts, Phys. Rev. D **52**, 5229 (1995); D. Ebert, V. O. Galkin and R. N. Faustov, Phys. Rev. D **57**, 5663 (1998); Y. S. Kalashnikova, A. V. Nefediev and Y. A. Simonov, Phys. Rev. D **64**, 014037 (2001); M. Di Pierro and E. Eichten, Phys. Rev. D **64**, 114004 (2001).
 - [7] G. S. Bali, Phys. Rev. D **68**, 071501 (2003); A. Dougall *et al.* (UKQCD Collaboration), Phys. Lett. B **569**, 41 (2003).
 - [8] T. Barnes, F. E. Close and H. J. Lipkin, Phys. Rev. D **68**, 054006 (2003); E. E. Kolomeitsev and M. F. M. Lutz, Phys. Lett. B **582**,

- 39 (2004); F. K. Guo, P. N. Shen, H. C. Chiang, R. G. Ping and B. S. Zou, Phys. Lett. B **641**, 278 (2006); D. Gamermann, E. Oset, D. Strottman and M. J. Vicente Vacas, Phys. Rev. D **76**, 074016 (2007); F. K. Guo, C. Hanhart and U. G. Meissner, Eur. Phys. J. A **40**, 171 (2009); M. Cleven, F. K. Guo, C. Hanhart and U. G. Meissner, Eur. Phys. J. A **47**, 19 (2011).
- [9] H. Y. Cheng and W. S. Hu, Phys. Lett. B **566**, 193 (2003); Y. Q. Chen and X. Q. Li, Phys. Rev. Lett. **93**, 232001 (2004); V. Dmitrasinovic, Phys. Rev. Lett. **94**, 162002 (2005).
- [10] E. V. Beveran and G. Rupp, Phys. Rev. Lett. **91**, 012003 (2003); K. Terasaki, Phys. Rev. D **68**, 011501 (2003); T. E. Browder, S. Pakvasa and A. A. Petrov, Phys. Lett. B **578**, 365 (2004); L. Maiani, F. Piccinini, A. D. Polosa and V. Riquer, Phys. Rev. D **71**, 014028 (2005); M. E. Bracco, A. Lozea, R. D. Matheus, F. S. Navarra and M. Nielsen, Phys. Lett. B **624**, 217 (2005); L. Liu, K. Orginos, F. K. Guo, C. Hanhart and U. G. Meissner, Phys. Rev. D **87**, 014508 (2013); D. Mohler *et al.* Phys. Rev. Lett. **111**, 222001 (2013); C. B. Lang *et al.*, Phys. Rev. D **90**, 034510 (2014).
- [11] B. Aubert *et al.* (BABAR Collaboration), Phys. Rev. D **74**, 032007 (2006).
- [12] S. Godfrey, Phys. Lett. B **568**, 254 (2003).
- [13] A. Faessler, T. Gutsche, V. E. Lyubovitskij and Y. L. Ma, Phys. Rev. D **76**, 014005 (2007); M. Cleven, H. W. Griehammer, F. K. Guo, C. Hanhart and U. G. Meiner, Eur. Phys. J. A **50**, 149 (2014).
- [14] K. Terasaki, Prog. Theor. Phys. Suppl. **186**, 141 (2010).
- [15] A. M. Torres, E. Oset, S. Prelovsek and A. Ramos, J. High Energ. Phys. **2015**, 153 (2015).
- [16] M. Ablikim *et al.* (BESIII Collaboration), Chin. Phys. C **39**, 093001 (2015).
- [17] M. Ablikim *et al.* (BESIII Collaboration), Chin. Phys. C **40**, 063001 (2016).
- [18] M. Ablikim *et al.* (BESIII Collaboration), Nucl. Instrum. Meth. A **614**, 345 (2010).
- [19] C. Zhang *et al.*, “Construction and commissioning of BEPCII”, Proc. PAC09, Vancouver, Canada(2009).
- [20] S. Agostinelli *et al.* (GEANT4 Collaboration), Nucl. Instrum. Meth. A **506**, 250 (2003).
- [21] Z. Y. Deng *et al.*, HEP & NP **30**, 371 (2006).
- [22] S. Jadach, B. F. L. Ward, and Z. Was, Comput. Phys. Commun. **130**, 260 (2000); Phys. Rev. D **63**, 113009 (2001).
- [23] E. Barberio and Z. Was, Comput. Phys. Commun. **79**, 291 (1994).
- [24] D. J. Lange, Nucl. Instrum. Meth. A **462**, 152 (2001).
- [25] R. G. Ping, Chin. Phys. C **32**, 599 (2008).
- [26] G. Balossini, C. M. Carloni Calame, G. Montagna, O. Nicrosini and F. Piccinini, Nucl. Phys. B **758**, 227 (2006).
- [27] J. C. Chen, G. S. Huang, X. R. Qi, D. H. Zhang and Y. S. Zhu, Phys. Rev. D **62**, 034003 (2000).
- [28] M. J. Oreglia, Ph.D. Thesis, SLAC-236 (1980); J. E. Geiser, Ph.D. Thesis, Stanford University, SLAC-R-255 (1982); T. Skwarnicki, Ph.D. Thesis, DESY F31-86-02 (1986).
- [29] M. Ablikim *et al.* (BESIII Collaboration), Phys. Rev. D **91**, 112005 (2015).
- [30] M. Ablikim *et al.* (BESIII Collaboration), Phys. Rev. D **87**, 012002 (2013).
- [31] E. Prencipe *et al.* (PANDA Collaboration), EPJ Web Conf. **95**, 04052 (2015).